Can highly non-polar low molecular weight polyisobutylenes be measured by electrospray ionization mass spectrometry? Anion-attachment provides an appropriate method for their characterization

Lajos Nagy[1], Tibor Nagy[1], György Deák[1], Ákos Kuki[1], Mihály Purgel[2], Mijid Narmandakh[3], Béla Iván[3], Miklós Zsuga[1] and Sándor Kéki[1]*

[1]*Department of Applied Chemistry, University of Debrecen, H-4032 Debrecen, Egyetem tér 1, Hungary*

[2]*Department of Physical Chemistry MTA-DE Homogeneous Catalysis and Reaction Mechanisms Research Group, University of Debrecen, H-4032 Debrecen, Egyetem tér 1, Hungary*

[3]*Polymer Chemistry Research Group, Institute of Materials and Environmental Chemistry, Research Center for Natural Sciences, Hungarian Academy of Sciences, H-1117 Budapest, Magyar Tudósok krt. 2, Hungary*

Abstract

Polyisobutylenes (PIBs) with different end-groups including chlorine, *exo*-olefin, hydroxyl and methyl initiated from aliphatic and aromatic initiator were studied by electrospray ionization mass spectrometry (ESI-MS). Independently of the end-groups, presence or absence of aromatic initiator moiety, these PIB derivatives were capable of forming adduct ions with NO_3^- and Cl^- ions, and thus allowing the direct characterization of these compounds in the negative ion mode of ESI-MS. To obtain $[PIB+NO_3]^-$ and $[PIB+Cl]^-$ adduct ions with appreciable intensities, addition of polar solvents such as acetone, 2-propanol or ethanol, to the dichloromethane solution of PIBs was necessary. Furthermore, increasing the polarity, i.e., increasing the acetone content in the acetone/dichloromethane mixtures and the ion-source temperature give rise to enhanced intensities for both $[PIB+NO_3]^-$ and $[PIB+Cl]^-$ ions. Energy-dependent collision induced dissociation studies (CID) revealed that increasing the collision voltages resulted in the shift of the apparent molecular masses to higher ones. CID studies also showed that dissociation of the $[PIB+Cl]^-$ ions requires higher collision energy than that of the $[PIB+NO_3]^-$. In addition, high level quantum chemical calculations were performed to get deeper insight into the nature of the interactions between the highly non-polar PIB chains and anions NO_3^- and Cl^- as well as to determine the Gibbs free energies for the formations of $[PIB+NO_3]^-$ and $[PIB+Cl]^-$ adduct ions.

Introduction

Polyisobutylenes (PIBs) are non-polar hydrocarbon polymers produced only by cationic polymerization of isobutylene [1]. Owing to their hydrophobicity, excellent chemical resistance and biocompatibility PIBs find their application in many fields including coatings, lubricants, sealants [1] as well as biomaterials for various biomedical applications [2]. Low molecular weight PIBs are also frequently used as building blocks for making various amphiphilic block copolymers and conetworks. The knowledge of molecular weight and the end-groups of these blocks are essential for the synthesis of polymeric materials with well-defined structure and architecture [2-6]. Mass spectrometry especially those based on soft ionization technique such as matrix-assisted laser desorption ionization (MALDI-MS)[7,8] and electrospray ionization mass spectrometry (ESI-MS) [9] have become very popular for the determination of molecular weight and end-groups of different polymers [10,11]. However, one of main drawbacks of these mass spectrometric methods is that polymers only those have repeat unit and/or functional group capable of forming adduct ions with certain ions, e.g., H^+, Na^+, K^+, Cl^- or through deprotonation can be analyzed. Non-polar hydrocarbon polymers with saturated bonds and with no heteroatom are not (or not easily) amenable to MALDI-MS and ESI-MS. The development of new ion-sources such as atmospheric pressure photoionization (APPI) [12,13] and direct analysis in real-time (DART) [14] paved the way for the analysis of less polar compounds including the non-polar hydrocarbon polymers, too. In some previous reports, we have shown that APPI-MS is an appropriate method for the characterization of low molecular weight PIBs [15,16] and other non-polar polymers [17] through the formation of $[M+Cl]^-$ adduct ions. In these experiments the chloride ions were produced "in situ" from chlorinated solvents. In addition, very recently, we have also demonstrated the capability of DART-MS for the analysis of low molecular weight PIBs [18]. Although DART-MS and especially APPI-MS are well suited for the characterization of PIBs and other non-polar polymers these ion-sources are not common and thus may not be available for mass spectrometrists interested in the investigation of such non-polar polymers. Moreover, ESI-sources are available in most mass spectrometric laboratories but they are mainly applied for polar compounds. According to the literature to make the highly non-polar PIBs amenable to ESI-MS the presence of any polar group capable of forming adduct ions or deprotonation is necessary [19-21]. Albeit the above mentioned works represent important

2

steps towards the successful characterization of highly non-polar PIB derivatives by ESI-MS, these approaches do not seem to be generally applicable. In this article, we present a more general approach for the characterization of low molecular weight PIBs by ESI-MS which is based on the adduct ion formation of PIBs with nitrate and chloride ions. Since the anions (NO_3^- Cl^-), as will be shown by means of high level quantum chemical calculations, attach to the partially positively charged hydrogen atoms of PIBs, the end-group does not affect significantly the resulting ESI-MS spectra. Thus, using this method, highly non-polar, low molecular weight PIBs with fully saturated bonds can be analyzed.

Experimental

Chemicals

2-propanol (HPLC grade), methanol (HPLC grade), ethanol (HPLC grade) acetone (HPLC grade) and sodium nitrate were purchased from VWR International (Leuven, Belgium). Ammonium chloride and ammonium nitrate from Reanal (Budapest, Hungary) were used. Sodium chloride were received from Sigma-Aldrich (Taufkirchen, Germany). Dichloromethane (a.r. grade) were purchased from Molar Chemicals (Budapest, Hungary) and distillated before use.

Brief description of the synthetic procedures for the preparations of polyisobutylene derivatives

The structures, the number-average molecular weights (M_n) and the polydispersities (M_w/M_n) of the polyisobutylene derivatives determined by Gel Permeation Chromatography (GPC) and mass spectrometry (MS) are compiled in Table 1.

Table 1.

All of the polyisobutylenes were synthesized by living carbocationic polymerization. PIB1 was prepared by living cationic polymerization of isobutylene initiated by p-dicumylchloride (1,4-di-(2-chloro-2-propyl)-benzene)/BCl_3 initiating system similarly to that described in ref. 22. The resulting polymer was a (tertiary) chlorine-terminated telechelic polyisobutylene. Applying similar synthetic procedure for the synthesis of PIB2, the resulting chlorine-terminated telechelic polyisobutylene was dissolved in tetrahydrofurane and was heated at reflux in the presence of potassium *tert*-butoxide to yield telechelic polyisobutylene with *exo*-olefin end-groups (PIB2) [22]. The telechelic polyisobutylene with *exo*-olefin end-groups

obtained in another polymerization reaction was reacted with 9-BBN (9-Borabicyclo[3.3.1]nonane) followed by oxidation with H_2O_2 to obtain hydroxyl-telechelic polyisobutylene (PIB3) [23]. PIB4 was obtained by living cationic polymerization of isobutylene initiated by 2-chloro-2,4,4-trimethyl-pentane (TMPCl)/$TiCl_4$ initiating system [24]. The chlorine terminated PIB that was obtained by living cationic polymerization of isobutylene initiated also by the TMPCl/$TiCl_4$ initiating system was treated with $Al(CH_3)_3$ to result in polyisobutylene with methyl end-group (PIB5)

Sample preparation

The polyisobutylene samples were dissolved in mixtures of acetone and dichloromethane in volume ratios (V/V) ranging from 0/100 to 90/10 V/V for PIB3, PIB4 and PIB5, while 0/100 to 50/50 for PIB1 and PIB2 at a concentration of 0.1 mg/mL, respectively. In some experiments instead of acetone, 2-propanol and ethanol were used. In order to promote the formation of negatively charged adduct ions 20 μL of saturated solutions of NH_4NO_3 or NH_4Cl in acetone/dichloromethane 50/50 V/V was added to the sample solutions of 1 mL.

Electrospray Quadrupole Time-of-Flight MS/MS (ESI-Q-TOF)

A MicroTOF-Q type Qq-TOF MS instrument (Bruker Daltonik, Bremen, Germany) was used for the MS and MS/MS measurements. The instrument was equipped with an electrospray ion source where the spray voltage was 4 kV. N_2 was utilized as drying gas. The drying temperature was 200 °C and the flow rate was 4.0 L/min. For the MS/MS experiments, nitrogen was used as the collision gas. The pressure in the collision cell was determined to be 1.2×10^{-2} mbar. The precursor ions for MS/MS were selected with an isolation width of 5 *m/z* units. The mass spectra were recorded by means of a digitizer at a sampling rate of 2 GHz. The mass spectra were calibrated externally using the exact masses of clusters $[(NaTFA)_n+TFA]^-$ generated from the electrosprayed solution of sodium trifluoroacetate (NaTFA). The spectra were evaluated with the DataAnalysis 3.4 software from Bruker. The sample solutions were introduced either directly into the ESI source with a syringe pump (Cole-Parmer Ins. Co., Vernon Hills, IL, USA) at a flow rate of 10 μL/min or by using a bypass loop for injecting 20 μL sample solution injected into the carrier solvent flow at a flow rate of 100 μL/min (**F**low **I**njection **A**nalysis).

.

Gel Permeation Chromatography (GPC)

Gel Permeation Chromatograms were recorded in THF at a flow rate of 0.5 mL/min at 35 $^{\circ}$C with a Waters chromatograph equipped with four gel columns (4.6 x 300 mm, 4.6 x μm Styragel columns: HR 0.5, 1, 2 and 4), a Waters Alliance 2695 HPLC pump and with a Waters 2414 refractive index detector. To obtain the number-average (M_n) and weight-average molecular weights (M_w) the GPC was calibrated using polystyrene standards of known molecular weights and narrow polydispersities.

Quantum Chemical Calculations

We performed DFT calculations with the B3LYP exchange-correlation functional [25]. Where 6-31G(d) were the standard split-valence basis sets [26]. Geometry optimizations were carried out *in vacuo*. Counterpoise calculations were also done to obtain BSSE correction for the anion-ligand interaction. All calculations were done using the Gaussian 09 software package [27]. The lack of imaginary frequencies in vibrational spectral calculations was taken to verify that the calculated stationary points on the potential energy surfaces (PES) represented true minima. The reported relative energies in this work are derived from the calculated zero-point corrected electronic energies of the corresponding structures.

Results and Discussion

ESI-MS of polyisobutylene derivatives recorded in the negative ion mode

As noted above, due to the very non-polar nature of polyisobutylenes (PIBs) and thus lack of effective ionization sites in PIBs capable of forming positively or negatively charged adducts with certain ions these polymers are very difficult to analyze by ESI-MS. Indeed, in the positive ion mode of ESI-MS no formation of adduct ions were observed when the PIB samples were mixed with salts containing different cations such as Na^+, K^+, NH_4^+ etc. However, in the negative ion mode of ESI-MS formations of $[PIB+NO_3]^-$ and $[PIB+Cl]^-$ adduct ions were seen when salts of nitrate or chloride were added to the PIB samples. Thus, PIBs with different end-groups and/or initiator moieties (listed in Table 1) were detected in the negative ion mode of ESI-MS. As a representative example, Fig. 1 shows the negative ion ESI-MS spectrum of PIB1, i.e., a chlorine-terminated telechelic polyisobutylene containing aromatic initiator moiety.

Fig. 1

As seen in Fig. 1, the main series is due to the presence of [PIB1+NO₃]⁻ adduct ions and the mass difference between the adjacent peaks is 56 matching the mass of an isobutylene unit. The highest detectable [PIB1+NO₃]⁻ ion appeared at $m/z \approx 2030$. In addition, as seen in the inset of Fig. 1, the experimental isotopic distribution is also in good agreement with the calculated one. Furthermore, comparisons of the observed and calculated m/z values also support the presence of PIB oligomers with the compositions corresponding to PIB1 (Table 1, line 1). For example, the measured and the calculated m/z values for the [PIB1+NO₃]⁻ adduct ion with a total number of isobutylene units of 13 are 1020.864 and 1020.865, respectively (The composition for this adduct ion is $C_{64}H_{120}Cl_2NO_3$). The additional low intensity series is due to the PIB1 ionized by the Cl⁻ ions. The appearance of these low intensity series can be attributed most probably to the ubiquitous presence of Cl⁻ ions in the solvents. It was intriguing to know whether the presence of polar group is essential for the ionization of PIBs. Thus, PIB with similar structure and molecular weight to PIB1 but with *exo*-olefin end-groups (PIB2) was further studied. It was found that PIB2 can easily be ionized by NO₃⁻ and Cl⁻ ions, too. The ESI-MS spectra of PIB2 recorded in the negative ion mode in the presence of NO₃⁻ and Cl⁻ ions can be found in the Supporting Information (Fig. S1, Fig. S2). Polyisobutylene with aromatic initiator moiety and hydroxyl end-groups (PIB3) showed also adduct ion formation with NO₃⁻ and Cl⁻ ions under ESI-MS conditions. The negative ion ESI-MS spectra of PIB3 in the acetone/dichloromethane (50/50 V/V) mixture ionized with NO₃⁻ and Cl⁻ ions are compiled in the Supporting information (Fig. S3, Fig. S4) while that of the PIB3 dissolved in ethanol recorded in the presence of Cl⁻ ions is shown in Fig. 2.

Fig. 2.

It should be noted that there is no significant difference in the relative ESI-MS distribution when acetone/dichloromethane mixture or ethanol are used as solvents. The effect of the solvent polarity on absolute ESI-MS intensity will be discussed later. Moreover, when ethanol was used low intensity but well-defined series of peaks appeared in the range of m/z 1800-2900 (Fig. 2 inset). These peaks, according to the accurate mass measurement, are due to the formation of [2PIB3+NaCl₂]⁻ ions as shown in Fig. 2 inset. Albeit formations of dimers (and trimers, etc) are frequently observed in ESI-MS. Such kind of adduct consisting of highly non-polar polymer and a complex $NaCl_2^-$ components to the best of our knowledge has not been described yet.

In the next series of experiments, in order to find out whether the aromatic initiator moiety is necessary for PIBs to be ionized by NO_3^- ions, PIB4 with chlorine end-group and without aromatic initiator moiety was subjected to ESI-MS investigations. Fig. 3 shows that PIB4 can indeed be ionized by NO_3^- ions to obtain ESI-MS spectrum.

Fig. 3.

As shown in Fig. 3 the measured isotopic distributions are in line with the calculated ones as well as the measured and the calculated *m/z* values are also in good agreement, e.g. the measured *m/z* for PIB4 with n=18 is 1107.093 while the calculated for the composition of $C_{72}H_{145}ClNO_3$ is 1107.092. The two additional low intensity series of peaks are due to the presence of [PIB4+Cl]$^-$ and [PIB4-HCl+NO$_3$]$^-$ ions. This latter series is formed by elimination of HCl molecule from PIB4 either under ESI-MS conditions or during the work-up of the polymer sample.

However, one of the most challenging issues in ESI-MS analysis is the soft ionization of highly non-polar hydrocarbon polymers with fully saturated bonds and absence of any heteroatom. As it can be seen in Fig. 4, ionization of such polymers can be achieved under ESI-MS conditions as the example of PIB5 shows. PIB5, is a fully saturated hydrocarbon polymer and does not contain any heteroatom but it can be effectively ionized by NO_3^- ions.

Fig. 4.

Both the measured isotopic distribution and the *m/z* values are in good agreement with the theoretical ones, e.g. for the composition of $C_{61}H_{124}NO_3$ (n=15) the measured and the calculated masses are 918.957 and 918.959, respectively. The two additional, low intensity series of peaks are due to the PIB5 ionized by Cl$^-$ ions and the presence of the small fraction of chlorine terminated polyisobutylene ionized by NO_3^- ions. This latter polymer series present in the sample as unreacted starting material from which PIB5 was synthesized by treating the chlorine-terminated PIB with $Al(CH_3)_3$.

.

Dependence of the ESI-MS intensity on the solvent polarity and the ion-source temperature

When pure dichloromethane, which is a good solvent for the low molecular weight PIBs investigated, was used for the ESI-MS experiments, very weak or no ESI-MS signals were obtained. On the contrary, when mixtures of dichloromethane and the more polar acetone, 2-propanol or ethanol were applied, appreciable negative ion ESI-MS signals appeared. It should be kept in mind, however, that very polar solvents can not be used because the PIBs owing to their non-polar character are insoluble in these polar solvents. To study how the ESI-MS intensity depends on the solvent composition, PIBs were dissolved dichloromethane-acetone mixtures in different compositions using constant NH_4NO_3 concentration. Fig. 5 shows the variations of the ESI-MS intensities with the compositions of dichloromethane-acetone mixtures for the PIB3 and PIB4 samples ionized by NO_3^- ions.

Fig. 5.

As it turns out from Fig. 5, in pure dichloromethane and at low acetone content (up to 10 % V/V) no significant ESI-MS intensities are observed. Further increasing the amount of acetone in the solvent mixture the ESI-MS intensities start to increase considerably for both PIB3 and PIB4. Moreover, in the case of PIB1 ESI-MS intensities continuously grow up to 90 % V/V acetone content, while in the case of PIB4 above 60 % V/V acetone content a slight decrease in the ESI-MS intensity can be observed. To interpret tentatively the observed ESI-MS *versus* acetone content curves we consider eq. 1 which is an approximate equation for the electrospray current (I) derived by Fernandez de la Mora and Locertales for highly conducting liquids [28].

$$I = f(\varepsilon_r)\sqrt{\gamma \kappa V_F \varepsilon_r} \qquad (1)$$

where f(ε_r), ε_r, γ, κ and V_F are a numerical function, the relative permittivity, surface tension, electric conductivity and the flow rate, respectively.

In our case, as going from dichloromethane to acetone the relative permittivity increase from 9 to 21, while the surface tensions of dichloromethane and acetone are very similar 27.2 and 23.5 mN/m, respectively [29]. Furthermore, it can also be expected that the conductivity at

constant salt concentration also increase as the permittivity of the solvent (or solvent mixture) increases due to the more effective dissociation of salts into free, solvated ions in more polar solvents. Hence, increase in the ion current, and thus in the ESI-MS intensity of the analyte may be expected with the increasing amount of acetone in the solvent mixture in good qualitative agreement with eq. 1. The slight decrease in the ESI-MS intensity in the case of PIB4 above 60 % V/V acetone content may be attributed to the lower solubility of PIB4 as compared to that of PIB1 in acetone. During evaporation of the solvent(s) the electrosprayed droplets become more concentrated in acetone due to the lower boiling point of dichloromethane. Thus, PIB4 partly precipitates out in the droplet leaving less "free" PIB4 chains to "escape" into the gas-phase after consecutive droplet fissions.

The dependence of the ESI-MS intensity on the temperature of the ion-source was also investigated. Fig. 6a shows the changes of the ESI-MS intensities with the ion-source temperatures for the $[PIB3+NO_3]^-$ ion formed from solvent mixtures of acetone/dichloromethane and 2-propanol/dichloromethane, while in Fig 6.b the variations of the relative ESI-MS intensities with the ion-source temperatures are plotted.

Fig. 6.

As seen in Fig. 6a raising the ion-source temperature favours the formation of $[PIB3+NO_3]^-$ adduct ion, i.e., higher ESI-MS intensities are obtained at higher ion-source temperatures, although a slight decrease with the increasing temperature in the range of 100-150 ^{o}C was observed for the 2-propanol/dichloromethane mixture. The fact that the ESI-MS intensities increase with the ion-source temperature may be attributed to the more effective desolvation process at higher temperatures. On the other hand, based on Fig. 6a, it can also be surmised that PIB3 in 2-propanol/dichloromethane mixtures gives lower ESI-MS intensities at the same ion-source temperatures than in acetone/dichloromethane mixtures especially in the range of 120-220 ^{o}C. This finding may be due to the facts that 2-propanol has higher boiling point (82 ^{o}C) as compared to that of acetone (56 ^{o}C) [29], thus lower boiling point provides more effective desolvation for the analyte at the same ion-source temperatures. On the other hand, it is likely that difference in the permittivity of the solvent mixtures does not play a significant role in the enhanced ESI-MS intensity obtained from acetone/dichloromethane with respect to 2-propanol/dichloromethane solution as the permittivity of the acetone (21) and 2-propanol (20) are very similar [29]. Furthermore, it is important and is evident from Fig. 6b that the

ion-source temperature does not affect the resulting ESI-MS intensity distribution in the range of 100-225 °C.

Dependence of the number-average molecular weight on the collision cell voltage

As discussed, NO_3^- and Cl^- ions can be attached to PIB chains under electrospray conditions to form the corresponding adduct ions. The negatively charged anions are most likely ligated to the partially positively charged hydrogen atoms of PIB chains as we have assumed based our earlier APPI-MS and DART-MS results obtained on related topics. Although in our recent ESI-MS investigations saturated solution of salts (thus, their concentrations were unknown) were used to facilitate the ionization of PIBs, it was found that PIBs with NO_3^- ions appeared with higher intensity than PIBs with Cl^- ions. Indeed, when NH_4NO_3 and NH_4Cl were dissolved in methanol at known concentrations, mixed in equimolar ratio and added to the solutions of PIBs the resulting ESI-MS spectrum revealed that $[PIB+NO_3]^-$ adduct ions occurred with ca. 3-4 times higher intensity than $[PIB+Cl]^-$ adduct ions. This finding may highlight the fact that the surface concentration NO_3^- ions is higher than that of the Cl^- ions. The reason for that is most likely due to the higher surface activity of NO_3^- ions as compared to that of Cl^- ions.

In order to obtain information on the energetics of $[PIB+NO_3]^-$ and $[PIB+Cl]^-$ adduct ions the collision energy was varied in the normal MS mode. Note that certain collision energy, typically 5-8 eV, is necessary to transfer the ions into the TOF part of the Q-TOF MS instrument. As seen in Fig. 7a by increasing the collision voltage from 8 eV to 22 eV considerable shift in the ESI-MS intensity distribution to higher masses can be observed.

Fig. 7.

The shift to higher masses with the increasing collision energies can be ascribed to the dissociation of lower mass adduct ions into neutral polymers molecule and anions. The preferential dissociation of lower molecular weight PIB adduct ions to that of higher ones is most likely due to the so-called degrees of freedom (DOF) effect. According to this at a given collision energy, the internal energy shared for fragmentation of the dissociating bond is higher for the lower mass ions, as compared to that of the higher ones bringing about that lower mass ion, i.e., with lower DOF value, dissociate in the time frame of MS experiments. In order to rule out that the shifts are not due to the effects such mass dependent scattering of the ions in the collision cell or any other mass discrimination issues we selected

10

polypropylene glycol (PPG) with similar molecular weight to that of the PIBs cationized by Li^+ ions. Li^+ ions forms adduct with PPG with relative high activation energy for fragmentation [30], thus $[PPG+Li]^+$ adduct ions do not fragment significantly neither by losing cation nor backbone cleavages in the collision energy range of 8-30 eV. In this experiment we used the same parameter set as in the negative ion mode by reversing the polarity. According to this experiment, no shift in the ESI-MS intensity distribution was observed, indicating the absence of mass discrimination effect and supporting that the shifts of intensity distribution to higher masses are caused by the DOF effect. On the other hand, from the finding that the PIB adduct ions dissociate at relatively low collision energies it can be concluded that the activation energy for fragmentation is relatively low. The shift of the ESI-MS intensity distribution as a function of the collision energy can also be modelled by using an Arrhenius type reaction rate constant. The details and the results of this approach can be found in the Supporting Information (Fig. S5, Fig. S6).

The other consequence of the intensity distribution shift to higher masses with the increasing collision energy is that the number-average molecular weights (M_n) calculated from the corresponding ESI-MS intensities as outlined in legend to Fig. 7 also increases. In Fig. 7b the variation of the M_n values with the collision energy for the $[PIB4+NO_3]^-$ and $[PIB4+Cl]^-$ ions are plotted. As seen in Fig. 7b the apparent M_n values increases closely linearly with the collision energy for both $[PIB4+NO_3]^-$ and $[PIB4+Cl]^-$ ion and the values of M_n at low collision energy (8-12 eV) are practically the same. However, the apparent M_n values for the $[PIB4+NO_3]^-$ increase more steeply than for the $[PIB4+Cl]^-$ adduct ion. This finding indicates that the dissociation energy of the adduct ion into a neutral polymer molecule and an anion is lower for the $[PIB4+NO_3]^-$ than for the $[PIB4+Cl]^-$ adduct ion. This observation was further supported by means of energy-dependent collision induced dissociation (CID) MS/MS experiments in which the $[PIB4+NO_3]^-$ and the $[PIB4+Cl]^-$ adduct ion with the same number of repeat unit were selected simultaneously using a relative wide mass window. It was found, in good agreement with the above mentioned finding, that the signal of the $[PIB4+NO_3]^-$ decreased to a greater extent with respect to that of the $[PIB4+Cl]^-$ adduct ion. Similar experiences were obtained for the other PIB derivatives, too, namely dissociation of the $[PIB+Cl]^-$ requires higher energy than that of the $[PIB+NO_3]^-$ ion. Figure representing the variation of the relative intensities of $[PIB4+NO_3]^-$ and $[PIB4+Cl]^-$ is available in the Supporting Information (Fig. S7).

At this point it is worth comparing the data of Table 2, in which the M_n values of the PIBs determined by GPC and ESI-MS are summarized.

Table 2.

As seen in Table 2 for PIB3 and PIB4 GPC and ESI-MS yielded very similar M_n and M_w/M_n values. However, for the M_n of PIB5 ESI-MS gave higher values than GPC. The higher M_n value determined by ESI-MS can be ascribed to the dissociation of lower molecular weight adduct ions (lower DOF values) in the ion-source and/or during transmission through the collision cell giving rise to an increase in the M_n value. Furthermore it can also be concluded from the data of Table 2 that M_n of PIB1 and PIB2 determined by ESI-MS are considerably lower than those by GPC. Note that M_w/M_n–s of both PIB1 and PIB2 are higher than 1.3 so these samples represent relatively broad molecular weight distribution from the MS point of view. Thus, due to the mass discrimination effect, MS are less sensitive to the higher mass polymer fraction, hence, the presence of higher molecular weight fraction of the distribution is under estimated based on the ESI-MS intensities.

Quantum Chemical Calculations

DFT calculations were performed to gain insight into the interaction between PIB and small anions such as chloride and nitrate. For these calculations, PIB5 oligomers with different molecular weights including 240, 352, 464 and 576 g/mol corresponding to total numbers of isobutylene units 4, 6, 8 and 10, respectively, were selected. In the calculations, the different conformers were also taken into account. The relative energies for the conformers and the Gibbs free energies for the various adduct ions are summarized in the Table 3.

Table 3.

According to the data of Table 3 the open straight *chain* conformation is more favored energetically than the *gauche* one. The *chain-gauche* conformation effect was observed for the PIB-n10 and PIB-n6 oligomers but this effect for the smaller, PIB-n4 oligomer was negligible. On the contrary, the relative energies for the conformers revealed opposite orders when they interacted with the anions because the *gauche* conformer builds a "cage" for the anions resulting in a greater number of energetically favorable hydrogen atom-anion interactions.

We have also performed calculations for a third possible conformer of the PIB-n10 oligomer In this conformation, the oligomer is *half opened* and there is a *gauche* region (n = 6) in the

middle part of the oligomer. According to these calculations, although all the interactions between the isobutylene units and the anions are energetically preferred, moreover, these interactions, due to the opposite trends in the relative energies of the oligomers and the adduct ions, are more favorable in the *gauche* conformation.

It is also evident from the data of Table 3. that there are no significant differences in the Gibbs free energies for the formations of adduct ions PIB-n6-chloride-*gauche*, PIB-n8-chloride-*gauche* and PIB-n10-chloride-*gauche* (ca. 60 kJ/mol). Similar observation but lower Gibbs free energy values can be established for the adduct ions PIB-n6-nitrate-*gauche*, PIB-n8-nitrate-*gauche* and PIB-n10-nitrate-*gauche* (ca. 47 kJ/mol). However, the Gibbs free energies for the formations of adduct ions PIB-n4-chloride-*gauche* and PIB-n4-nitrate-*gauche* are lower than their larger size homologues (n6, n8 and n10) with values of ~15.0 kJ/mol and ~10.0 kJ/mol, respectively. Furthermore, PIB-n6 and PIB-n8, due to the similar alignment and the number of the hydrogen atom-anion interactions involved in the adduct ion formation, show very similar result to that obtained for the *half opened* conformer of PIB-n10. Fig. 8 shows the structures of conformers of PIB-n10 adduct ions with bonds H⋯Cl and H⋯O within bond lengths of 3 Å.

Fig. 8.

In the PIB-n10-chloride adduct ion there are 10 H⋯Cl bonds available for the *gauche* conformer while only 4 are for the *chain* conformer. Although in the PIB-n10-nitrate adduct ion the average H⋯O distances are ~30-40 pm shorter, moreover, the *gauche* conformer consists of a more complicated bond-system including 16 H⋯O bonds, while the nitrated *chain* conformer (PIB-n10-nitrate-*chain*) is similar to the chlorinated one (PIB-n10-chloride-*chain*).

On the other hand, the *gauche* conformer of PIB-n10 enwraps the anions fully. Thus, PIB-n10 may be regarded as a critical, lowest sized oligomer to obtain the highest stabilization effect for the adduct ion formation. Evidently, for the higher sized homologues neither the Gibbs free energy for the adduct ion formation nor the "wrapping ability" of the PIB oligomer chains towards the anions will not change. It is also important to note that the Gibbs free energies for adduct ion formations are higher with the chloride ion than with nitrate in every cases by a value of ~10-15 kJ/mol. This finding is in line with the experimental results obtained by collision induced studies, namely, higher collision energies are needed for the dissociations of [PIB+Cl]⁻ ions than those of the [PIB+NO₃]⁻ ions. In addition, according to

our experience, the dissociation of PIB adduct ions of similar molecular weight (i.e. similar DOF values) to that of protonated leucine enkephalin ([Leu+H]$^+$) requires much lower collision energies than that of 100 kJ/mol. The activation energy for the fragmentation of [Leu+H]$^+$ is *ca* 100 kJ/mol [31], thus it may be concluded from the CID studies that dissociation energies of the PIB adduct ions are lower than 100 kJ/mol in good agreement with the results of quantum chemical calculations (see Table 3).

Conclusions

It was demonstrated with examples of polyisobutylene (PIB) derivatives having different end-groups, the presence and absence of aromatic initiator moiety that PIBs are capable of adduct ion formation with anions such as NO_3^- and Cl^- under electrospray conditions. This finding extends the capability of ESI-MS to the analysis of non-polar polar polymers and makes this method valuable when other ion-sources that are more appropriate for the investigation of non-polar compounds such as APPI-MS are not available. However, according to our experience, to obtain ESI-MS spectra of good quality in the negative mode for PIBs, solvent mixtures containing a polar solvent including acetone or 2-propanol should be applied. Another important conclusion of our work gained from the energy-dependent CID studies (in the normal MS and MS/MS modes) is that the dissociation energy for the [PIB+NO$_3$]$^-$ and [PIB+Cl]$^-$ ions may be relatively low and this finding was further supported by high level quantum chemical calculations. Thus, low molecular weight fraction of the adduct ions may decompose during the transmission, while the higher molecular weight part can survive owing to DOF effect, causing an apparent increase in the value of M_n. Thus, it is advisable that in the Q-TOF instrument the collision voltage should be kept as low as possible. On the other hand, PIBs with higher polydispersities ($M_w/M_n > 1.3$) can also be analyzed by ESI-MS, but in that case the M_n value determined based on the corresponding ESI-MS intensities are lower than those obtained by GPC. Based on our energy-dependent CID MS and MS/MS investigations it was also shown that bond dissociation energy for the [PIB+Cl]$^-$ is higher than for the [PIB+NO$_3$]$^-$ ion being in line with the results of high level quantum chemical calculations. Moreover, in spite of this fact, PIBs with NO_3^- ion gave ESI-MS spectra of higher quality than with Cl^- ion. Furthermore, the anion attachment technique presented for PIBs in this report may be applicable to other non-polar polymers, too.

Acknowledgement

References

1. J.P. Varion, N. Spassky, Industrial Cationic Polymerizations: An Overview In Cationic Polymerizations: Mechanism, Synthesis, and Applications. Marcel Dekker, New York, Basel, Hong Kong (1996)

2. J.E. Puskas, Y. Chen, Biomedical application of commercial polymers and novel polyisobutylene-based thermoplastic elastomers for soft tissue replacement, Biomacromolecules 5 (2004) 1141-1154.

3. B. Iván, K. Almdal, K. Mortensen, I. Johannsen, J. Kops, Synthesis, characterization, and structural investigations of poly(ethyl acrylate)-l-polyisobutylene bicomponent co-network, Macromolecules. 34 (2001) 1579–1585.

4. M. Burkhardt, M. Ruppel, S. Tea, M. Drechsler, R. Schweins, D.V. Pergushov, M. Gradzielski, A.B. Zezin, A.H.E. Müller, Water-soluble interpolyelectrolyte complexes of polyisobutylene-block-poly(methacrylic acid) micelles: Formation and properties, Langmuir 24, (2008) 1769–1777.

5. J.P. Kennedy, G. Fenyvesi, R.P. Levy, K.S. Rosenthal, Amphiphilic networks. XV. Amphiphilic membranes with controlled mesh dimensions for insulin delivery, Macromol. Symp. 172 (2001) 56–66.

6. J. Yun, R. Faust, Sz.L. Szilágyi, S. Kéki, M. Zsuga, Effect of architecture on the micellar properties of amphiphilic block copolymers: Comparison of AB linear diblock, A1A2B, and A2B heteroarm star block copolymers, Macromolecules 36 (2003) 1717-1723.

7. M. Karas, F. Hillenkamp, Laser desorption ionization of proteins with molecular masses exceeding 10,000 Daltons, Anal. Chem. 60 (1988) 2299–2301.

8. K. Tanaka, H. Waki, Y. Ido, S. Akita, T. Yoshida, Protein and polymer analyses up to m/z 100,000 by laser ionization time-of-flight mass spectrometry, Rapid Commun. Mass Spectrom. 2 (1988) 151–153.

9. S.F. Wong, C.K. Meng, J.B. Fenn, Multiple charging in electrospray ionization of poly(ethylene glycols), J. Phys. Chem. 92 (1988) 546–550.

10. L. Li, ed., MALDI mass spectometry for synthetic polymer analysis, John Wiley & Sons, Inc., Hoboken, New Jersey (2010)

11. G. Montaudo, R.P. Lattimer, ed., Mass spectometry of polymers, CRC press, Taylor & Francis Group, Boca Raton, FL (2002)

12. D. Robb, T. Covey, A. Bruins, Atmospheric pressure photoionization: An ionization method for liquid chromatography-mass spectrometry, Anal. Chem. 72 (2000) 3653–3659.

13. J.A. Syage, M.D. Evans, K.A. Hanold, Photoionization mass spectrometry, Am. Lab. 32 (2000) 24–29.

14. R.B. Cody, A.J. Laramée, H.D. Durst, Versatile new ion source for the analysis of materials in open air under ambient conditions, Anal. Chem. 8 (2005) 2297-2302.

15. S. Kéki, J. Török, L. Nagy, M. Zsuga, Atmospheric pressure photoionization mass spectrometry of polyisobutylene derivatives, J. Am. Soc. Mass Spectrom. 19 (2008) 656-665.

16. L. Nagy, V. Pálfi, M. Narmandakh, Á. Kuki, A. Nyíri, B. Iván, M. Zsuga, S. Kéki, Dopant-assisted atmospheric pressure photoionization mass spectrometry of polyisobutylene derivatives initiated by mono- and bifunctional initiators, J. Am. Soc. Mass Spectrom. 20 (2009) 2342-2351.

17. S. Kéki, L. Nagy, Á. Kuki, M. Zsuga, A new method for mass Spectrometry of polyethylene waxes: The Chloride Ion Attachment Technique by Atmospheric Pressure Photoionization, Macromolecules 41 (2008) 3772.

18. L. Nagy, T. Nagy, Gy. Deák, Á. Kuki, B. Antal, M. Zsuga, S. Kéki, Direct analysis in real time mass spectrometry (DART-MS) of highly non-polar low molecular weight polyisobutylenes, J. Mass Spectrom. 50 (2015) 1071–1078.

19. J.J. Harrison, C.M. Mijares, M.T. Cheng, J. Hudson, Negative ion electrospray ionization mass spectrum of polyisobutenylsuccinic anhydride: Implications for isobutylene polymerization mechanism, Macromolecules 35 (2002) 2494-2500.

20. E. Rivera-Tirado, D.J. Aaserud, C. Wesdemiotis, Characterization of polyisobutylene succinic anhydride chemistries using mass spectrometry, J. Appl. Polym. Sci. 124 (2012) 2682-2690.

21. K.M. Wollyung, C. Wesdemiotis, A. Nagy, J.P. Kennedy, Synthesis and mass spectrometry characterization of centrally and terminally amine-functionalized polyisobutylenes, J. Polym. Sci. Polym. Chem. 43 (2005) 946-958.

22. S. Kéki, M. Nagy, Gy. Deák, A. Lévai, M. Zsuga, Dimethyldioxirane as a new and effective oxidation agent for the epoxidation of α,ω-di(isobutenyl)polyisobutylene: A convenient synthesis of α,ω-di(2-methyl-3-hydroxypropyl)-polyisobutylene, J. Polym. Sci. Polym. Chem. Ed. 40 (2002) 3974–3986.

23. B. Iván, J.P. Kennedy, V.S.C. Chang, New telechelic polymers and sequential copolymers by polyfunctional *ini*tiator-trans*fer* agents (inifers). VII. Synthesis and characterization of α,ω-di(hydroxy)polyisobutylene, J. Polym. Sci. Polym. Chem. Ed. 18 (1980) 3177–3191.

24. G. Kaszás, J.E. Puskás, J.P. Kennedy, C.C. Chen, Electron-pair donors in carbocationic polymerization 3. carbocationic stabilization by external electron-pair donor sin isobutylene polymerization, J. Macromol. Sci. Chem. A26 (1989) 1099-1114.

25. Y. Zhao, D.G. Truhlar, The M06 suite of density functionals for main group thermochemistry, thermochemical kinetics, noncovalent interactions, excited states, and transition elements: two new functionals and systematic testing of four M06-class functionals and 12 other functionals, Theor. Chem. Acc. 120 (2008) 215-241.

26. W.J. Hehre, R. Ditchfield , J.A. Pople, Self—Consistent Molecular Orbital Methods. XII. Further Extensions of Gaussian—Type Basis Sets for Use in Molecular Orbital Studies of Organic Molecules, J. Chem. Phys. 56 (1972) 2257.

27. M. J. Frisch, G. W. Trucks, H. B. Schlegel, G. E. Scuseria, M. A. Robb, J. R. Cheeseman, G. Scalmani, V. Barone, B. Mennucci, G. A. Petersson, H. Nakatsuji, M. Caricato, X. Li, H. P. Hratchian, A. F. Izmaylov, J. Bloino, G. Zheng, J. L. Sonnenberg, M. Hada, M. Ehara, K. Toyota, R. Fukuda, J. Hasegawa, M. Ishida, T. Nakajima, Y. Honda, O. Kitao, H. Nakai, T. Vreven, J. A. Montgomery, J. E. Peralta, F. Ogliaro, M. Bearpark, J. J. Heyd, E. Brothers, K. N. Kudin, V. N. Staroverov, R. Kobayashi, J. Normand, K. Raghavachari, A. Rendell, J. C. Burant, S. S. Iyengar, J. Tomasi, M. Cossi, N. Rega, N. J. Millam, M. Klene, J. E. Knox, J. B. Cross, V. Bakken, C. Adamo, J. Jaramillo, R. Gomperts, R. E. Stratmann, O. Yazyev, A. J. Austin, R. Cammi, C. Pomelli, J. W. Ochterski, R. L. Martin, K. Morokuma, V. G. Zakrzewski, G. A. Voth, P. Salvador, J. J. Dannenberg, S. Dapprich, A.

28. J. Fernandez de la Mora, I.G. Locertales, The current emitted by highly conducting Taylor cones. J. Fluid Dyn. 260 (1994) 155–184.

29. D.R. Lide, ed., CRC Handbook of Chemistry and Physics, CRC Press, Boca Raton, FL (2005)

30. Á. Kuki, G. Shemirani, L. Nagy, B. Antal, M. Zsuga, S. Kéki, Estimation of activation Energy from the survival yields: fragmentation study of leucine enkephalin and polyethers by tandem mass spectrometry, J. Am. Soc. Mass Spectom. 24 (2013) 1064-1071.

31. J. Sztaray, A. Memboeuf, L. Drahos, K. Vekey, Leucine enkephalin-a mass spectrometry standard, Mass Spectrom. Rev. 30 (2011) 298-320.

Legends for the Schemes and Figures

Fig. 1.

ESI-MS spectrum of PIB1 ionized by NO_3^- ions. The numbers at the top of the peaks stand for the total number of isobutylene units (n). The additional series of peaks denoted by asterisk is due to the PIB1 ionized by Cl^- ions. The inset shows the measured and the calculated isotopic distributions for [PIB1+NO_3]$^-$ adduct ion with a total number of isobutylene units 13. The composition for this adduct ion is $C_{64}H_{120}Cl_2NO_3$.

Fig. 2.

ESI-MS spectrum of PIB3 ionized by Cl^- ions. The inset shows the presence of [2M+$NaCl_2$]$^-$ adduct ions. The numbers at the top of the peaks stand for the total number of isobutylene units (n). Solvent: ethanol.

Fig. 3.

ESI-MS spectrum of PIB4 ionized by NO_3^- ions. The numbers at the top of the peaks stand for the total number of isobutylene units (n). The additional series of peaks denoted by asterisk and sign "+" are due to the PIB4 ionized by Cl^- ions and presence of [PIB4-HCl+NO_3]$^-$ adduct ions, respectively. The inset shows the measured and the calculated isotopic distributions for [PIB4+NO_3]$^-$ adduct ion with n=18. The composition for this adduct ion is $C_{72}H_{145}ClNO_3$.

Fig. 4.

ESI-MS spectrum of PIB5 ionized by NO_3^- ions. The numbers at the top of the peaks stand for the total number of isobutylene units (n). The additional series of peaks denoted by asterisk and sign "+" are due to the PIB5 ionized by Cl^- ions and presence of the chlorine terminated polyisobutylene ionized by NO_3^- ions, respectively. The inset shows the measured and the calculated isotopic distributions for [PIB5+NO_3]$^-$ adduct ion with a total number of isobutylene units 15. The composition for this adduct ion is $C_{61}H_{124}NO_3$.

Fig. 5.

The dependence of the ESI-MS intensities of the [PIB3+NO_3]$^-$ (**a**) and [PIB4+NO_3]$^-$ (**b**) adduct ions on the composition of the acetone/dichloromethane mixture.

Fig. 6.

The dependence of the ESI-MS intensities of the [PIB3+NO_3]$^-$ adduct ions formed from acetone/dichloromethane (50/50 V/V) and 2-propanol/dichloromethane (50/50 V/V) solvent mixtures on the ion-source temperature (**a**) and variation of the ESI-MS intensities with the ion-source temperatures (solvent: acetone/dichloromethane 50/50 V/V) (**b**).

Fig. 7.

Shift of the ESI-MS intensity distribution with the collision energy for the [PIB4+NO_3]$^-$ adduct ions (**a**). Variation of the number-average molecular weights (M_n) calculated based on the corresponding ESI-MS intensities of the [PIB4+NO_3]$^-$ and [PIB4+Cl]$^-$ adduct ions with the collision energy (**b**). Solvent: acetone/dichloromethane 50/50 V/V.

Fig. 8.

The structures of the *chain* and the *gauche* conformers of PIB-n10-chloride and PIB-n10-nitrate adduct ions with bonds H···Cl and H···O within bond lengths of 3 Å.

Table 1. The structures of the polyisobutylene derivatives investigated.

Sample	Structure
PIB1	$$CH_3-\underset{CH_3}{\overset{CH_3}{C}}-CH_2-\left(\underset{CH_3}{\overset{CH_3}{C}}-CH_2\right)_x \underset{CH_3}{\overset{CH_3}{C}}-C_6H_4-\underset{CH_3}{\overset{CH_3}{C}}\left(CH_2-\underset{CH_3}{\overset{CH_3}{C}}\right)_y CH_2-\underset{CH_3}{\overset{CH_3}{C}}-Cl$$ with terminal Cl on left: $Cl-C(CH_3)_2-$
PIB2	$$CH_2\!\!=\!\!\underset{CH_3}{C}-CH_2-\left(\underset{CH_3}{\overset{CH_3}{C}}-CH_2\right)_x \underset{CH_3}{\overset{CH_3}{C}}-C_6H_4-\underset{CH_3}{\overset{CH_3}{C}}\left(CH_2-\underset{CH_3}{\overset{CH_3}{C}}\right)_y CH_2-\underset{CH_3}{C}\!\!=\!\!CH_2$$
PIB3	$$HO-CH_2-\underset{CH_3}{HC}-CH_2-\left(\underset{CH_3}{\overset{CH_3}{C}}-CH_2\right)_x \underset{CH_3}{\overset{CH_3}{C}}-C_6H_4-\underset{CH_3}{\overset{CH_3}{C}}\left(CH_2-\underset{CH_3}{\overset{CH_3}{C}}\right)_y CH_2-\underset{CH_3}{CH}-CH_2-OH$$
PIB4	$$CH_3-\underset{CH_3}{\overset{CH_3}{C}}-CH_2-\underset{CH_3}{\overset{CH_3}{C}}\left(CH_2-\underset{CH_3}{\overset{CH_3}{C}}\right)_m Cl$$
PIB5	$$CH_3-\underset{CH_3}{\overset{CH_3}{C}}-CH_2-\underset{CH_3}{\overset{CH_3}{C}}\left(CH_2-\underset{CH_3}{\overset{CH_3}{C}}\right)_m CH_3$$

Table 2. The number-average molecular weights (M_n) and the polydispersities (M_w/M_n) of the polyisobutylene derivatives determined by Gel Permeation Chromatography (GPC) and mass spectrometry (MS). The values of M_n and M_w were calculated based on the MS results as: $M_n = \Sigma I_i M_i / \Sigma I_i$ and $M_w = \Sigma I_i M_i^2 / \Sigma I_i M_i$, where I_i and M_i are the relative intensity and the mass of the oligomer with a number of repeat units i, respectively. M_w is the weight-average molecular weight.

Sample	M_n (GPC)	M_w/M_n (GPC)	M_n (MS)	M_w/M_n (MS)
PIB1	2160	1.40	1190	1.04
PIB2	2020	1.33	1390	1.04
PIB3	870	1.11	890	1.03
PIB4	1200	1.09	1170	1.03
PIB5	670	1.12	960	1.01

Table 3. ZPE corrected relative and Gibbs free energies for the investigated conformers of the PIB oligomers and adduct ions with anions NO_3^- and Cl^-. Basis Set Superposition Error (BSSE) corrected energies are collected for the adduct ions.

Conformer (ligand/complex)	Number of IB unit (n)	Relative energy of the conformers (kJ/mol)	Gibbs free energy for the adduct ion formation (kJ/mol)
PIB-n4-*chain*	4	0.0	−
PIB-n4-*gauche*	4	0.7	−
PIB-n4-chloride-*chain*	4	0.0	-36.0
PIB-n4-chloride-*gauche*	4	-7.3	-44.1
PIB-n4-nitrate-*chain*	4	0.0	-26.3
PIB-n4-nitrate-*gauche*	4	-7.6	-34.6
PIB-n6-*chain*	6	0.0	−
PIB-n6-*gauche*	6	6.2	−
PIB-n6-chloride-*gauche*	6	*	-59.0
PIB-n6-nitrate-*gauche*	6	*	-47.5
PIB-n8-*gauche*	8	*	−
PIB-n8-chloride-*gauche*	8	*	-58.8
PIB-n8-nitrate-*gauche*	8	*	-46.8
PIB-n10-*chain*	10	0.0	−
PIB-n10-*half opened*	10	5.1	−
PIB-n10-*gauche*	10	8.9	−
PIB-n10-chloride-*chain*	10	0.0	-42.0
PIB-n10-chloride-*half opened*	10	-11.4	-58.9
PIB-n10-chloride-*gauche*	10	-11.8	-62.3
PIB-n10-nitrate-*chain*	10	0.0	-31.6
PIB-n10-nitrate-*gauche*	10	-5.1	-45.6

* referred that only *gauche* conformer was investigated.

Fig. 1.
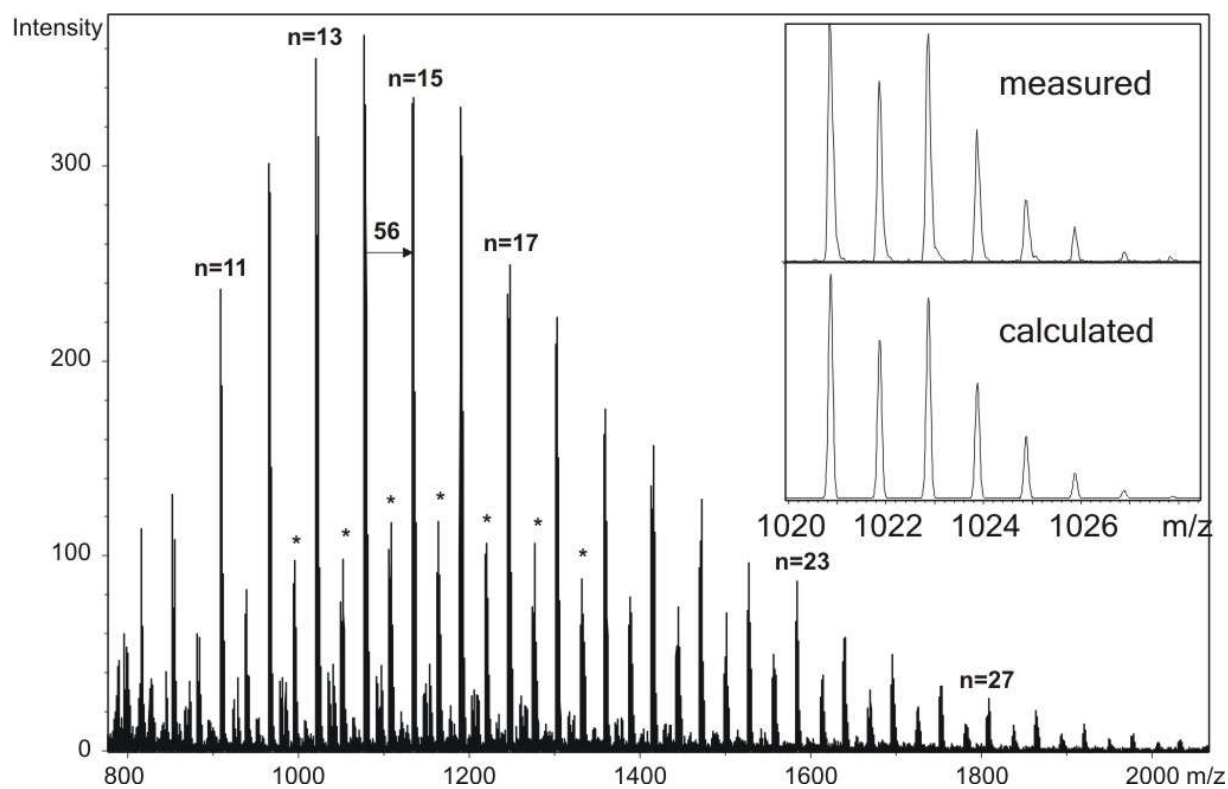
Fig. 2.
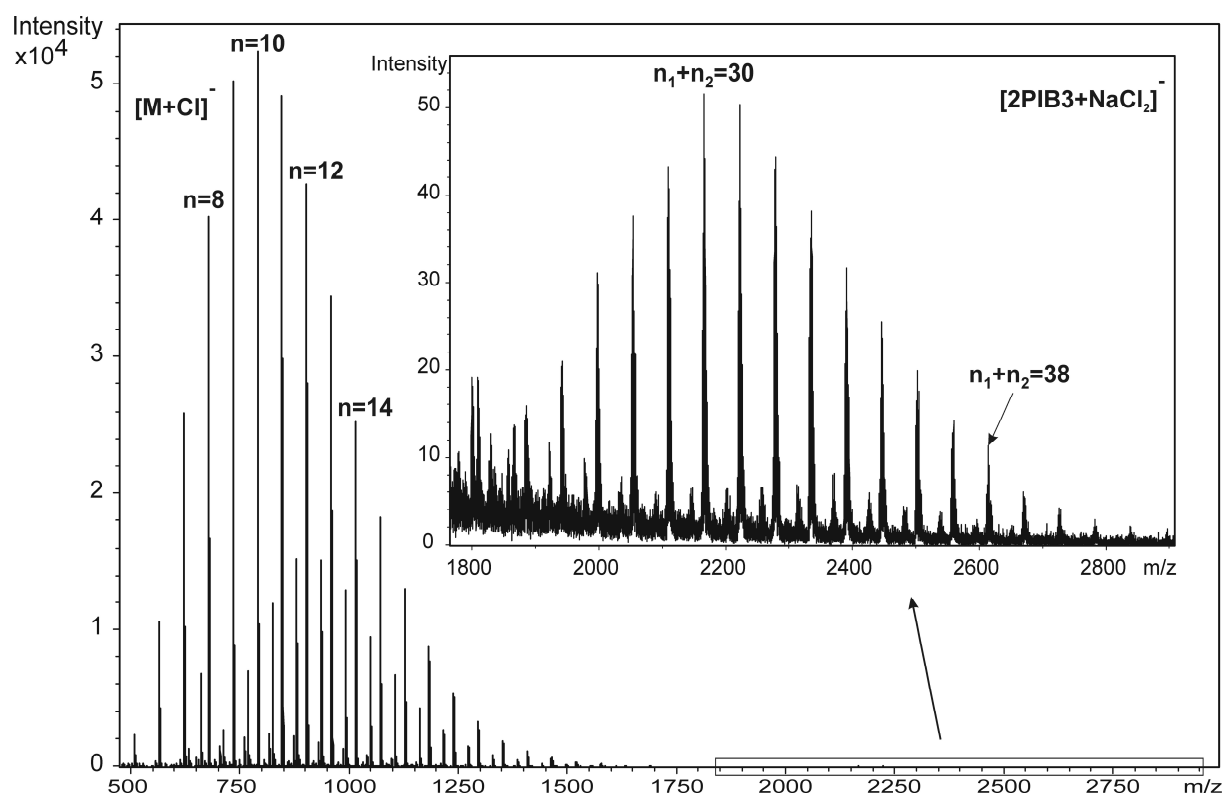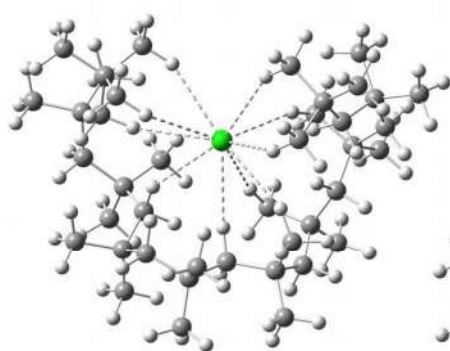
Fig. 3.
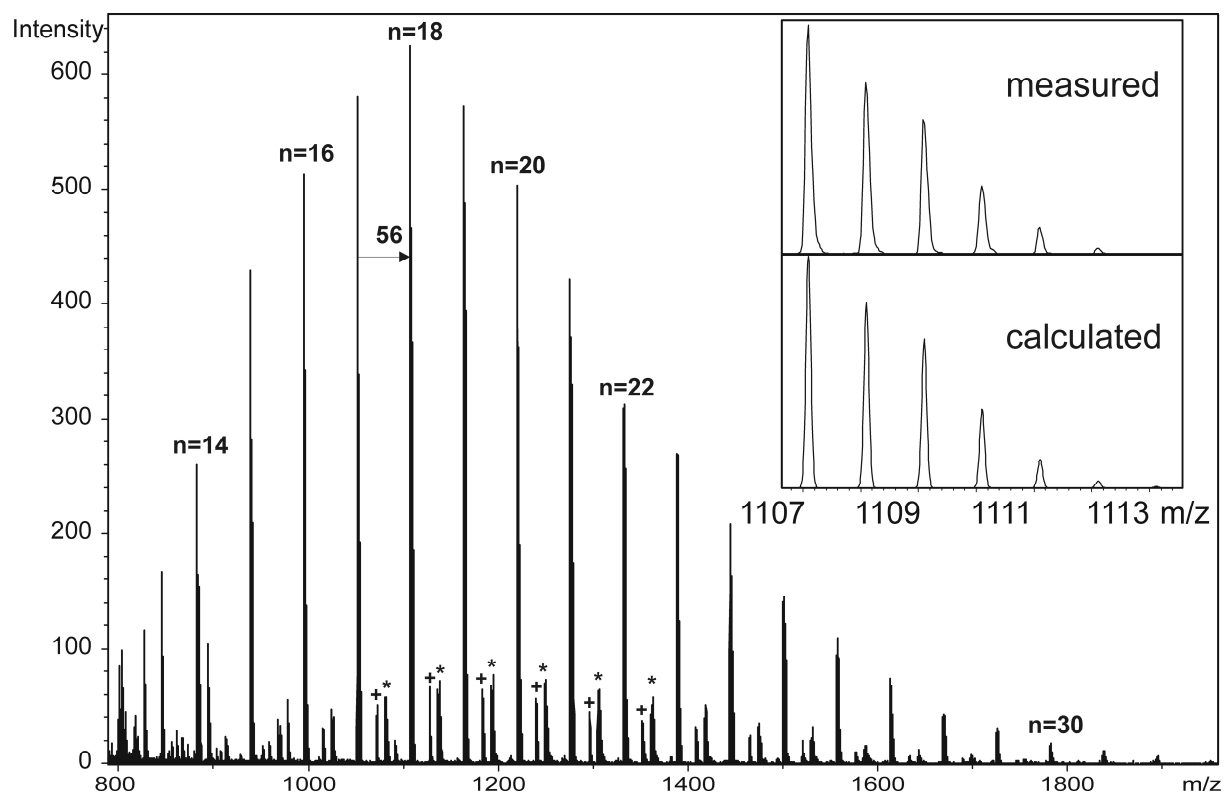
Fig. 4.
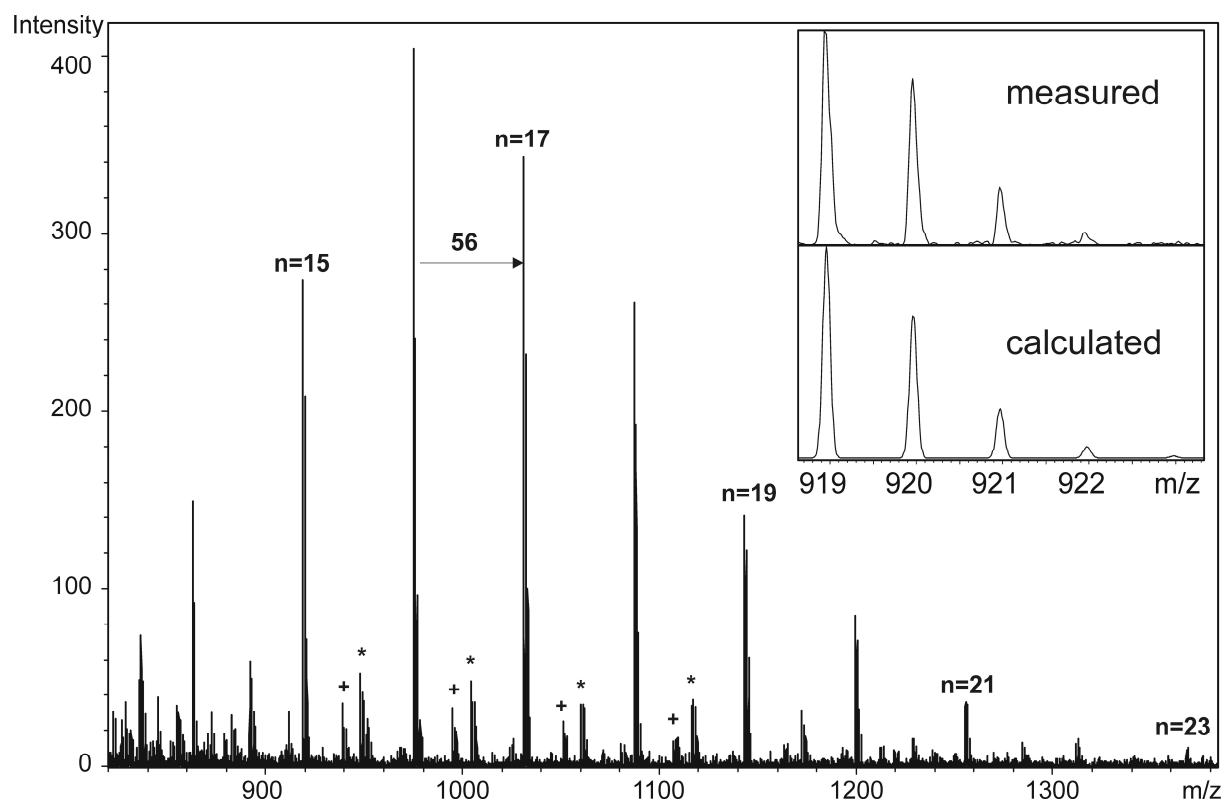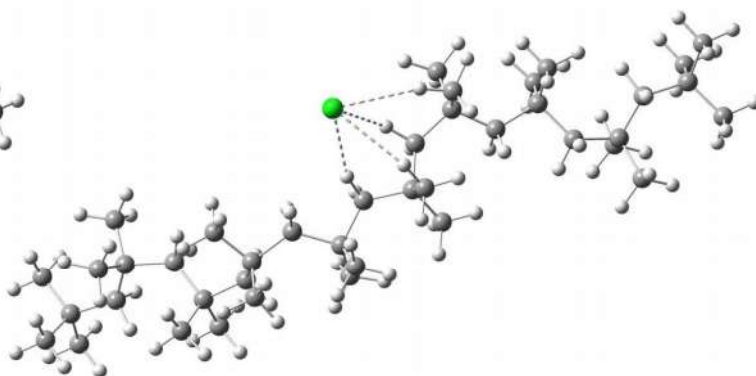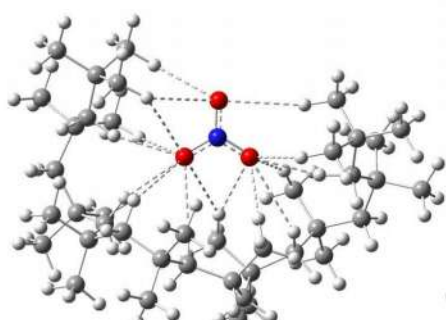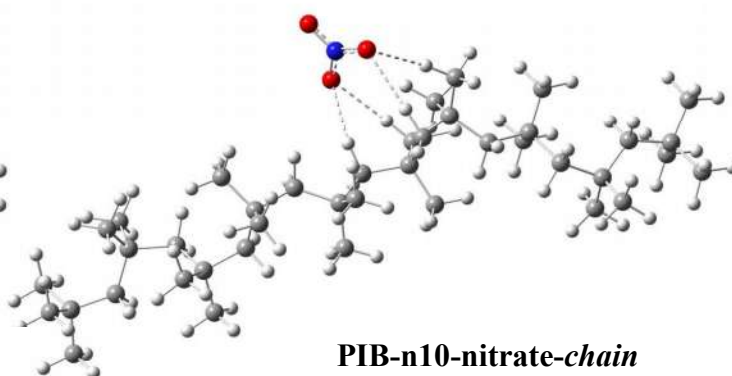
Fig. 5.
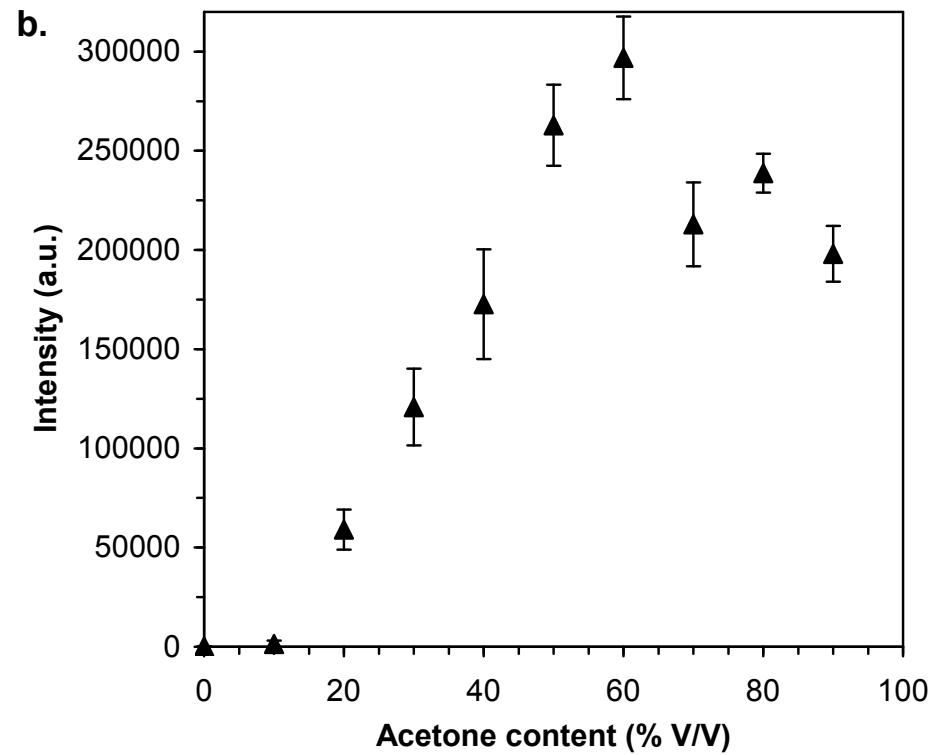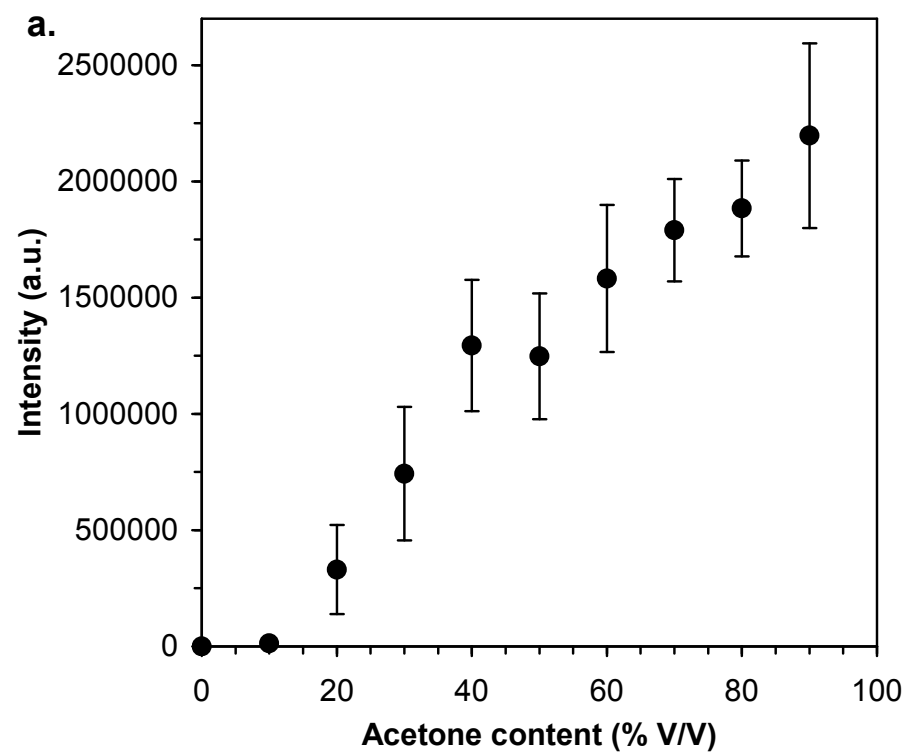
Fig. 6.
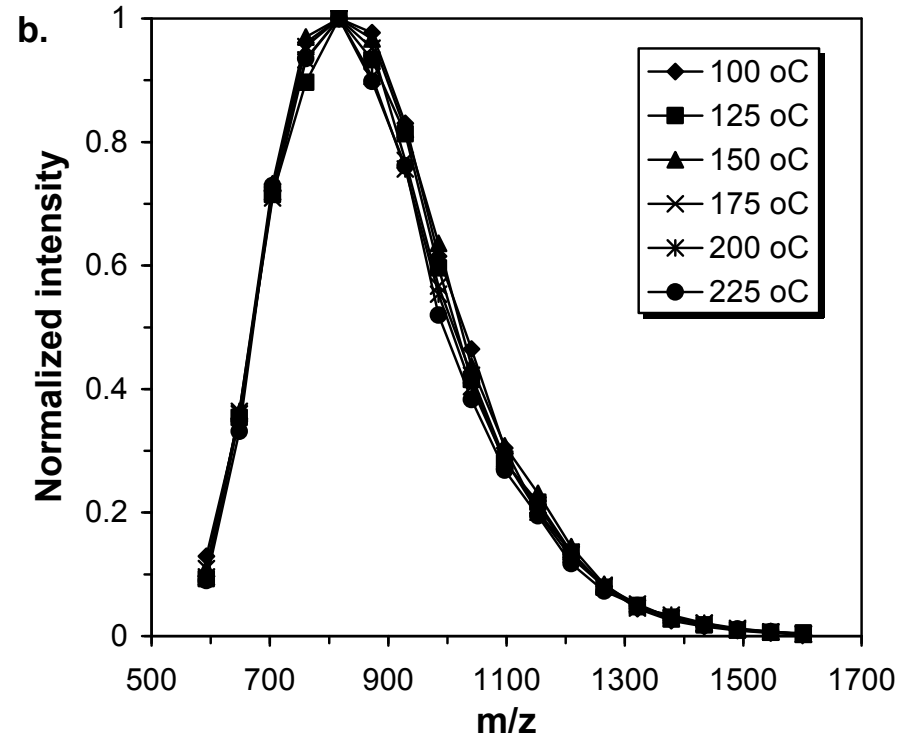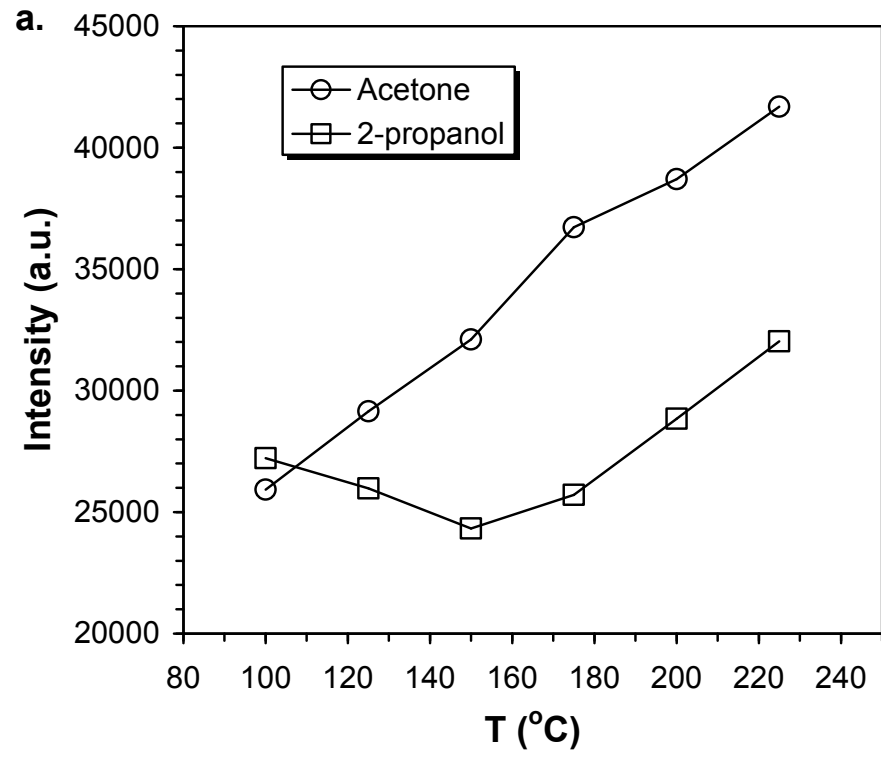
Fig. 7.
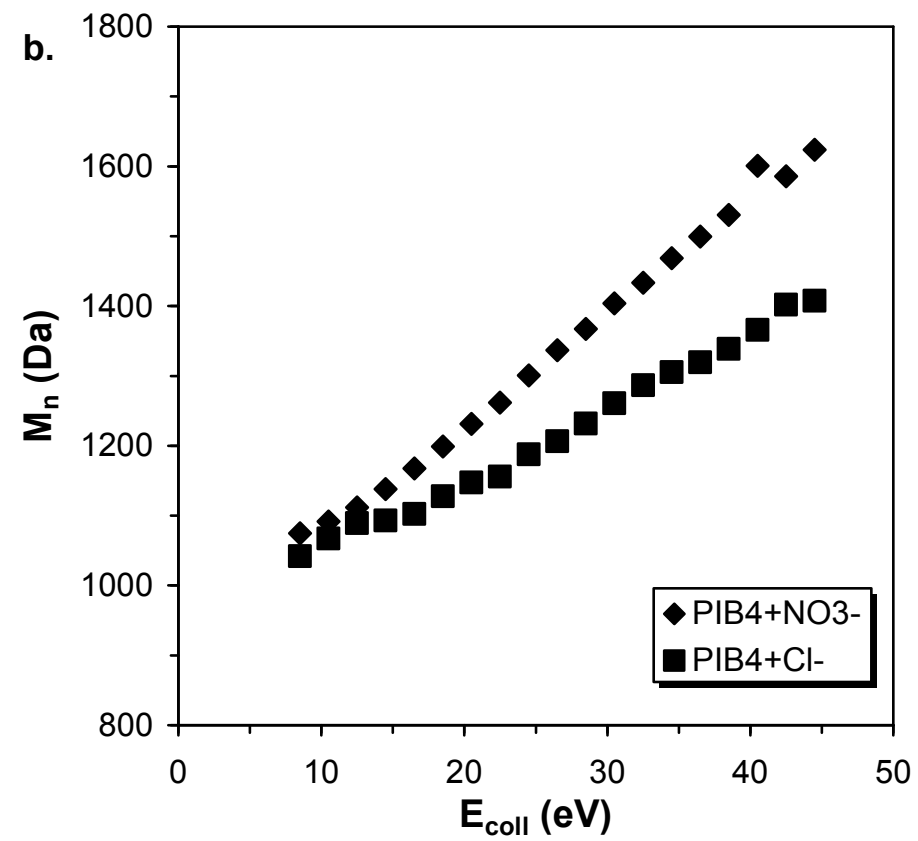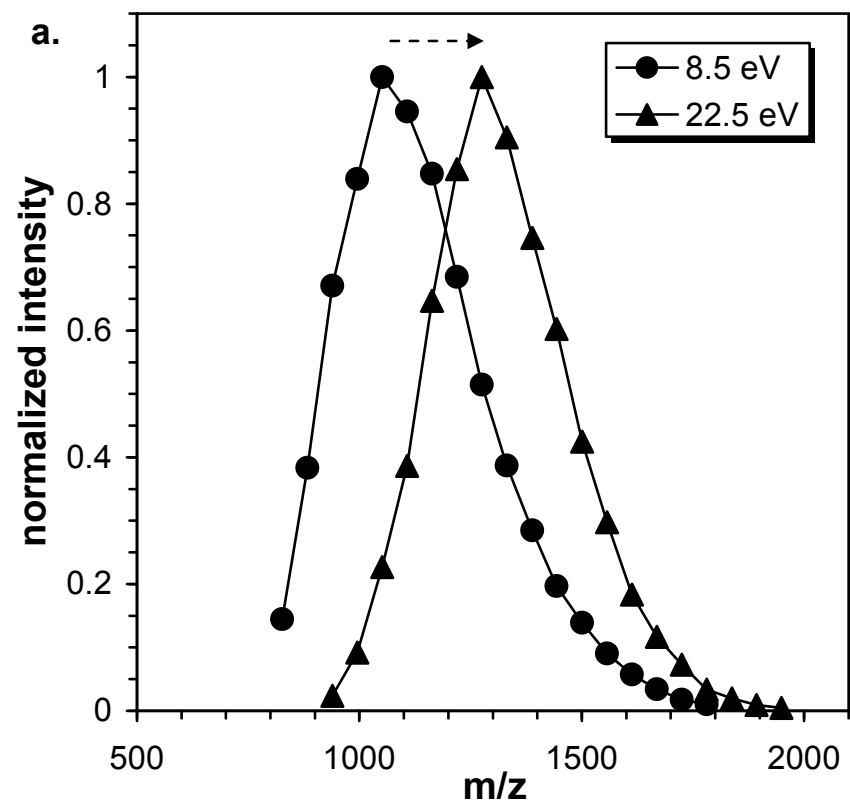
Fig. 8.

PIB-n10-chloride-*gauche*

PIB-n10-chloride-*chain*

PIB-n10-nitrate-*gauche*

PIB-n10-nitrate-*chain*